



# Indoor inhalation dose assessment for thoron-rich regions of Indian Himalayan belt

Poonam Semwal<sup>1</sup> · Tarun Kumar Agarwal<sup>2</sup> · Kuldeep Singh<sup>1</sup> · Manish Joshi<sup>2</sup> · Gurupad Singh Gusain<sup>1</sup> · Bijay Kumar Sahoo<sup>2</sup> · Rakesh Chand Ramola<sup>3</sup>

Received: 5 March 2018 / Accepted: 29 November 2018 / Published online: 19 December 2018  
© Springer-Verlag GmbH Germany, part of Springer Nature 2018

## Abstract

$^{222}\text{Rn}$ ,  $^{220}\text{Rn}$ , and their decay products are significant contributors to background radiation dose. Their concentration level, pertaining exposure, and consequent dose are prime concerns in indoor environments. The present study was performed in 101 dwellings of different villages of Almora district situated in Kumaun hills of Indian Himalayan belt. Measurement of gases and decay products were made in three different types of dwellings (i.e., mud, cemented, and stone with plaster) in three seasons (winter, summer, and rainy). Concentration values for  $^{222}\text{Rn}$  and EERC were found to be varying in the order of winter > summer > rainy while obtained least in rainy season for the case of  $^{220}\text{Rn}$  and EETC. Concentration values for  $^{222}\text{Rn}$  and EERC were found to be lesser for cemented houses. Relative standard deviation of concentration values was found to be higher for the rainy season. Yearly averaged concentration values for  $^{222}\text{Rn}$ , EERC,  $^{220}\text{Rn}$ , and EETC were noted to be higher than the global averages but comparable to some Indian studies. Annual inhalation dose due to  $^{222}\text{Rn}$ ,  $^{220}\text{Rn}$ , and their progeny was found to be 0.55–4.71 mSv/year with an average value of  $2.36 \pm 0.83$  mSv/year. These values were measured for the first time in the study area and provide a link for future studies in the dwellings representing higher concentration values.

**Keywords** Radon · Thoron · EERC · EETC · Inhalation dose · Seasonal variation

## Introduction

Naturally occurring  $^{222}\text{Rn}$  (radon) and  $^{220}\text{Rn}$  (thoron) radionuclides belonging to U-238 and Th-232 decay series are generated in soil and building materials (UNSCEAR 2000). These non-reactive gases find their way to the atmosphere from the source term and may accumulate inside dwellings. Once in open environment, these gases form decay products which along with parent gases contribute almost half to the

background natural radiation dose (UNSCEAR 2000, 2010). Their concentration levels, pertaining exposure, and consequent dose are prime concerns in indoor environments (for both general population and occupational workers). On one hand, knowledge gathered towards  $^{222}\text{Rn}$  inhalation dosimetry has good and accurate understanding of facts such as dominant contribution of decay products to dose in comparison to gases and exposure-dose relationship (Br et al. 2012; Omori et al. 2016; Singh et al., 2016b; Ramola et al. 2016; Teras et al. 2016). On the other hand, several studies are conducted to understand other peripheral but crucial aspects e.g., concentration-ventilation relationships (Jelle 2012; Mishra et al. 2010; Vasilyev and Zhukovsky 2013), spatial distribution patterns (Barros-Diosa et al. 2007; Meisenberg et al. 2016), and validation/prediction models (Mishra et al. 2009a; Wang and Ward 2000). The outcome of any new measurement campaign imparts a contributory input to the existing knowledge framework. Important agencies, e.g., WHO (World Health Organization), UNSCEAR (United Nations Scientific Committee on the Effects of Atomic Radiation), and NSRP (National Symposium on Radiation Physics), also focus on the issue of  $^{222}\text{Rn}$  inhalation hazard

---

Responsible editor: Philippe Garrigues

✉ Manish Joshi  
mjoshi@barc.gov.in

<sup>1</sup> Department of Physics, Govt. P.G. College, New Tehri, Tehri Garhwal 249001, India

<sup>2</sup> Radiological Physics and Advisory Division, Bhabha Atomic Research Center, Mumbai 400094, India

<sup>3</sup> Department of Physics, HNB, Garhwal University, BadshahiThaul Campus, Tehri Garhwal 249199, India

by publishing reports and issuing guidelines for sensitizing public and government. Recently, the reference level of indoor  $^{222}\text{Rn}$  has been reduced from 200 to 100  $\text{Bq/m}^3$  (WHO 2009).

In recent times, lot of studies have been performed world-over focusing on the development of advanced instrumentation for measurement of concentration of indoor and outdoor  $^{222}\text{Rn}$ ,  $^{220}\text{Rn}$ , and their decay product concentration (Irlinger et al. 2014; Mayya et al. 2010; Mishra et al. 2008, 2009b; Park et al. 2018). Studies have also been conducted in this domain targeting development of models (Jelle et al. 2011, 2012; Jeon et al. 2017; Kumar et al. 2014; Sahoo et al. 2011) for specific contexts. In India, an exponential growth of similar studies can be noticed in the past two decades. Due to large variations in climatic conditions, socio-economic perspectives and geological influences; measurements performed at different regions/environmental conditions form an important basis for refined understanding of issues related to  $^{222}\text{Rn}/^{220}\text{Rn}$  inhalation dosimetry. Whereas average global indoor concentration of  $^{222}\text{Rn}$  and  $^{220}\text{Rn}$  is measured to be 40 and 10  $\text{Bq/m}^3$ , respectively (UNSCEAR 2000), these values may increase to 200  $\text{Bq/m}^3$  as well (Ramola et al. 2016). For India, a strong dependency of concentration levels with ventilation and source term has been highlighted (Mishra et al. 2009a; Sahoo and Mayya 2010). Wide differences in source term, climatic conditions, dwelling types, and ventilation patterns necessitate measurements in different environments. Studies have been conducted in hot as well as cold (Bajwa et al. 2016; Singh et al. 2016a; Prasad et al. 2015) environments, different dwelling types (Singh et al., 2016a; Singh et al., 2016b; Prasad et al., 2016a; Ramola et al. 2016; Sonkawade et al. 2008), and varying source term (Prasad et al. 2008a; Harris et al. 2006; Ryzhakova 2012; Sahoo and Mayya 2010) conditions. Additionally, studies such as exhalation potential of the source (Sahoo et al. 2010), soil depth profiling (Içhedef et al. 2013), and computational fluid dynamics-based predictions (Agarwal et al. 2016, 2014; Chauhan et al. 2015, 2014) have also been performed. The contribution of exposure from building materials is assumed to be negligible if they contain low radioactivity and exhalation rates than soil (Sahoo et al. 2011). The contribution of  $^{220}\text{Rn}$  for inhalation dosimetry in the Indian context has also been recognized (Joshi et al. 2010; Joshi et al. 2011; Ramola et al. 2010; Sahoo et al. 2014).

Although techniques are well established for the measurement of  $^{222}\text{Rn}/^{220}\text{Rn}$  gas, techniques and methodology for measuring decay product's concentration are still evolving. Deposition-based direct  $^{222}\text{Rn}/^{220}\text{Rn}$  progeny sensors (DRPS/DTPS) can be used for direct time-integrated measurement of decay product concentration (Mishra et al. 2009b; Mishra and Mayya 2008; Sharma et al. 2018). Exposure of decay products is estimated from the product of potential alpha energy concentration (PAEC) and exposure time. The conventional method of converting  $^{222}\text{Rn}$  concentration to PAEC (equilibrium factor approach) is limited due to the uncertainty in the equilibrium factors (Nikezic and Yu 2005). These decay products can be directly

measured employing DRPS/DTPS in terms of equilibrium equivalent concentrations (EECs). In comparison to  $^{222}\text{Rn}$ , indoor  $^{220}\text{Rn}$  concentration distribution is highly non-uniform. In such a case, single point gaseous measurements cannot be relied as summary indices representing the room conditions. By measuring decay products, DTPS avoids the uncertainty due to non-uniform concentration profile and relatively larger variation in equilibrium factor for  $^{220}\text{Rn}$ . Further equilibrium factors can be estimated using corroborated gaseous and decay product concentrations. Studies have shown that the equilibrium factor can be quite different from 0.4 and 0.02 (UNSCEAR 2008) provided for  $^{222}\text{Rn}$  and  $^{220}\text{Rn}$  dosimetry (Singh et al., 2016b; Prasad et al. 2016b; Ramola et al. 2003, 2016). It is important to assess variations in equilibrium factor for an unexplored region, preferably offering varied background conditions.

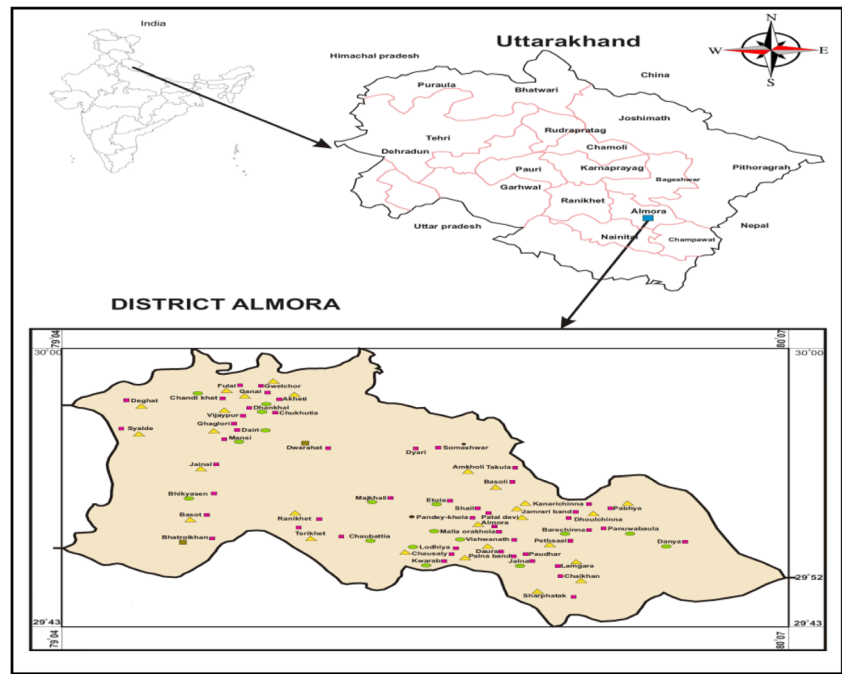
Field campaigns interpret the inferences based on the results obtained from measurements of indoor concentration levels. It is essential to expand the database by studying new regions/probing relevant issues. Indian Himalayan belt is one such region which is unique due to its geology, climate, and socio-economic perspectives (Singh et al. 2016a; Prasad et al. 2016a, b; Ramola et al. 2013, 2016). Studies performed in this belt (Singh et al. 2016a; Ramola et al., 2005; Prasad et al. 2015) have not covered the contributory factors responsible for maintaining indoor levels. Singh et al. 2016a measured  $^{222}\text{Rn}/^{220}\text{Rn}$  and decay products in Almora district of this belt for winter season only and underlined the need for extensive measurements for this thoron-rich region. This study presents results of a year-long measurement campaign conducted in Almora district of Kumaun Himalayan region, Uttarakhand, India. Activity concentration of  $^{222}\text{Rn}$ ,  $^{220}\text{Rn}$ , and their decay products was measured in 101 dwellings of differing construction materials situated at different villages. This study was conducted in three different seasons viz. winter, summer, and rainy. Yearly averaged concentration levels, dose calculations, seasonal variations, and dependencies on the type of construction material have been discussed. These first time elaborative results for this crucial Indian region provide a link for future studies apart from gaining useful understanding at present.

## Topography and experimental techniques

### Geology of study area and house statistics

This study was conducted in the dwellings of Almora district (latitude: 29°36' N, longitude: 79°30' E) in Kumaun Himalaya of Uttarakhand (Fig. 1). This hilly region is covered by the Himalayan range and its elevation varies from 750 to 1950 m with the average elevation of 1861 m above the sea level. The study area consists of highly mylonitised porphyritic, granite, quartz porphyry, schist phylites slates, and quartzites (Prasad et al. 2008b). The crystalline zone of Almora is divided into

**Fig. 1** Locations of all villages selected for measurements



two distinct lithologic units: (i) Sarju formation, represented by the porphyries, migmatites, schists, and micaceous quartzites; (ii) Duram formation represented by quartzites (Valdia 1963). The geology and composition of soil of this region are expected to be different from other regions of Himalayan belt. Apart from the geology, radioactive source term and emanation transport determine the exhalation potential of soil and rocks. Dwellings in Almora district are mostly made up by mud, stone with cement plaster, and brick with cement plaster. The mud houses are the oldest constructed dwellings as compared with stone with cement plaster and brick with cement plaster and are relatively poorly ventilated. In contrast, cemented houses are ventilated and constructed of concrete which includes calcite and some other minerals. A pre-survey for measuring outdoor gamma radiation levels was conducted covering the entire Almora district. Consequently, villages/blocks were segregated into three different groups/gamma radiation zones ( $\leq 0.01$ ,  $0.11\text{--}0.20$ , and  $\geq 0.20$   $\mu\text{Sv/h}$ ). A number of dwellings of different construction types (mud, stone with cement plaster, and brick with cement plaster) in each zone were then selected by ensuring statistical compliances. In all, a total of 101 dwellings categorized as mud houses, stone with cemented houses, and cemented houses were fixed for elaborative measurements (in villages shown in Fig. 1).

**Experimental techniques**

**Measurement of gas concentration**

Single entry pin-hole-based dosimeter technique, indigenously developed by Bhabha Atomic Research Centre (BARC), was

used for the measurement of indoor  $^{222}\text{Rn}$  and  $^{220}\text{Rn}$  concentrations (Sahoo et al. 2013). The schematic diagram for Pin-hole dosimeter is shown in Fig. 2. Through the single entry face, gas enters (through glass fiber filter paper) to the first chamber namely “ $^{222}\text{Rn} + ^{220}\text{Rn}$ ” compartment and subsequently diffuses (through pin holes) to the second chamber called “ $^{222}\text{Rn}$ ” chamber. The LR-115 detector films are fixed at the end of each compartment to register the track formed by alpha particle emitted from  $^{222}\text{Rn}$ ,  $^{220}\text{Rn}$ , and their decay products. The first compartment measures both  $^{222}\text{Rn}$  and  $^{220}\text{Rn}$  while the second measures only  $^{222}\text{Rn}$ . Details about this technique and device are discussed extensively in Sahoo et al. 2013. These devices (pin-hole dosimeters) have been used in several studies in recent past (Singh et al. 2016a; Meisenberg et al. 2016; Singh et al., 2016b; Ramola et al. 2016).

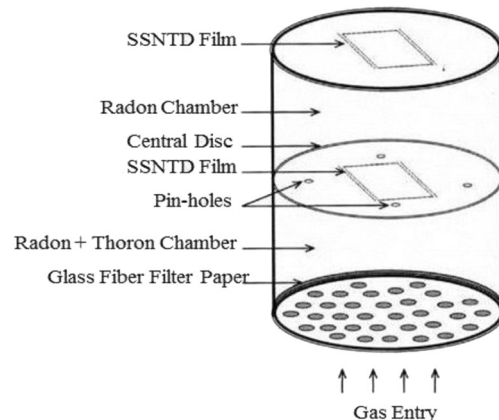


**Fig. 2** Schematic diagram of single entry pin-hole dosimeter

### Measurement of decay product concentration

Measurement of <sup>222</sup>Rn and <sup>220</sup>Rn decay product was carried out using Direct <sup>222</sup>Rn Progeny Sensor (DRPS) and Direct <sup>220</sup>Rn Progeny Sensor (DTPS), respectively. These devices comprise of LR115 detector film and an aluminized mylar coupled in a cassette-type assembly. The thickness (37 μm thickness for DRPS, 50 μm thickness for DTPS) of mylar is selected so as to register tracks due to alpha particles emitted from <sup>214</sup>Po (α energy 7.69 MeV) and <sup>212</sup>Po (α energy 8.78 MeV) in the case of <sup>222</sup>Rn progeny detection and from <sup>212</sup>Po (α energy 8.78 MeV) in the case of <sup>220</sup>Rn progeny detection (see Fig. 3).

Equilibrium equivalent concentration of the decay products in the air can be calculated from the tracks counted using sensitivity and calibration factors. Details of technique, calibration, and conversion factors can be found elsewhere (Mishra et al. 2010, 2009a, b; Mishra and Mayya 2008). These sensors have been routinely used in different studies in recent past (Bajwa et al. 2016; Singh et al. 2016a; Mishra et al. 2014; Singh et al. 2016b; Ramola et al. 2016).

### Estimation of equilibrium factors for <sup>222</sup>Rn and <sup>220</sup>Rn

Equilibrium equivalent concentration (EEC) of <sup>222</sup>Rn/<sup>220</sup>Rn is equal to that quantity of <sup>222</sup>Rn/<sup>220</sup>Rn which is in secular equilibrium with its decay products giving equivalent potential alpha energy concentration (PAEC) for the progeny nuclides actually present in the atmosphere. EERC and EETC used in the present context are the total EEC of <sup>222</sup>Rn and <sup>220</sup>Rn measured by DRPS and DTPS, respectively. The equilibrium factor is defined as the ratio of EERC/EETC to the <sup>222</sup>Rn/<sup>220</sup>Rn concentration in the environment. The equilibrium factors for <sup>222</sup>Rn (F<sub>Rn</sub>) and <sup>220</sup>Rn (F<sub>Tn</sub>) were calculated by using Eqs. (1) and (2) (UNSCEAR 2000).

$$F_{Rn} = \frac{EERC}{C_R} \tag{1}$$

$$F_{Tn} = \frac{EETC}{C_T} \tag{2}$$

where C<sub>R</sub> and C<sub>T</sub> are the concentrations of <sup>222</sup>Rn and <sup>220</sup>Rn, respectively, measured by the single entry pin-hole-based dosimeter.

### Estimation of total annual inhalation dose

The total annual inhalation dose (D/AID) due to the exposure of indoor <sup>222</sup>Rn, <sup>220</sup>Rn, and their progeny can be obtained from the following equation (UNSCEAR 2000, Ramola et al. 2016).

$$D(mSv/y) = \{(0.17 + 9 \times F_R) \times C_R + (0.11 + 40 \times F_T) \times C_T\} \times 8760 \times 0.8 \times 10^{-6} \tag{3}$$

On substituting the value of F<sub>Rn</sub> and F<sub>Tn</sub> from Eqs. (1) and (2), this equation gets converted to

$$AID(mSv/y) = (0.17 \times C_R + 9 \times EERC + 0.11 \times C_T + 40 \times EETC) \times 8760 \times 0.8 \times 10^{-6} \tag{4}$$

In the present study, the total annual inhalation dose (AID) due to the exposure of indoor <sup>222</sup>Rn, <sup>220</sup>Rn, and their progeny has been calculated by using Eq. (4).

Annual effective dose (AED) due to the exposure of <sup>222</sup>Rn, <sup>220</sup>Rn, and their progeny can be calculated by using Eqs. (5) and (6).

$$AED_R(mSv/y) = EERC (Bq/m^3) \times 8760 h \times 0.8 \times 9 nSv (Bq.h/m^3)^{-1} \times 10^{-6} \tag{5}$$

$$AED_T(mSv/y) = EETC (Bq/m^3) \times 8760 h \times 0.8 \times 40 nSv (Bq.h/m^3)^{-1} \times 10^{-6} \tag{6}$$

where EERC and EETC are the equilibrium equivalent concentrations of <sup>222</sup>Rn and <sup>220</sup>Rn, respectively, for the dwellings of the study area. The dose conversion factors are 0.17 and 9 for <sup>222</sup>Rn and its progeny concentrations and 0.11 and 40 for <sup>220</sup>Rn and its progeny concentrations, respectively (UNSCEAR 2000). The indoor occupancy factor was taken as 0.8 as for the study area (UNSCEAR 1993). The multiplication factor 10<sup>-6</sup> is used for unit conversion from

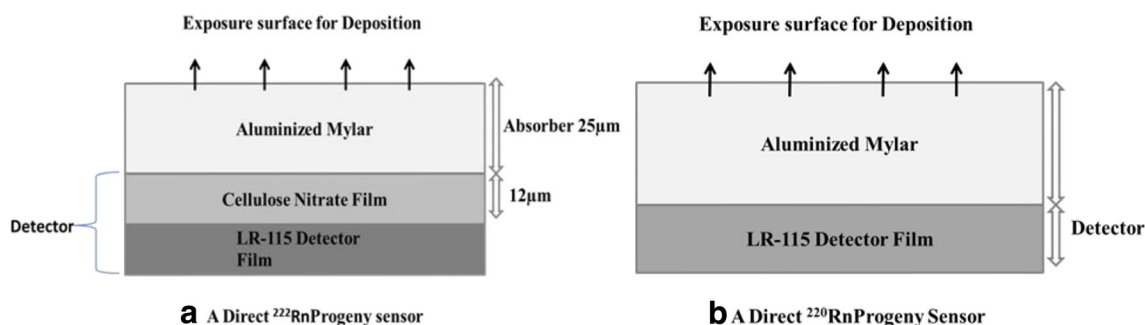
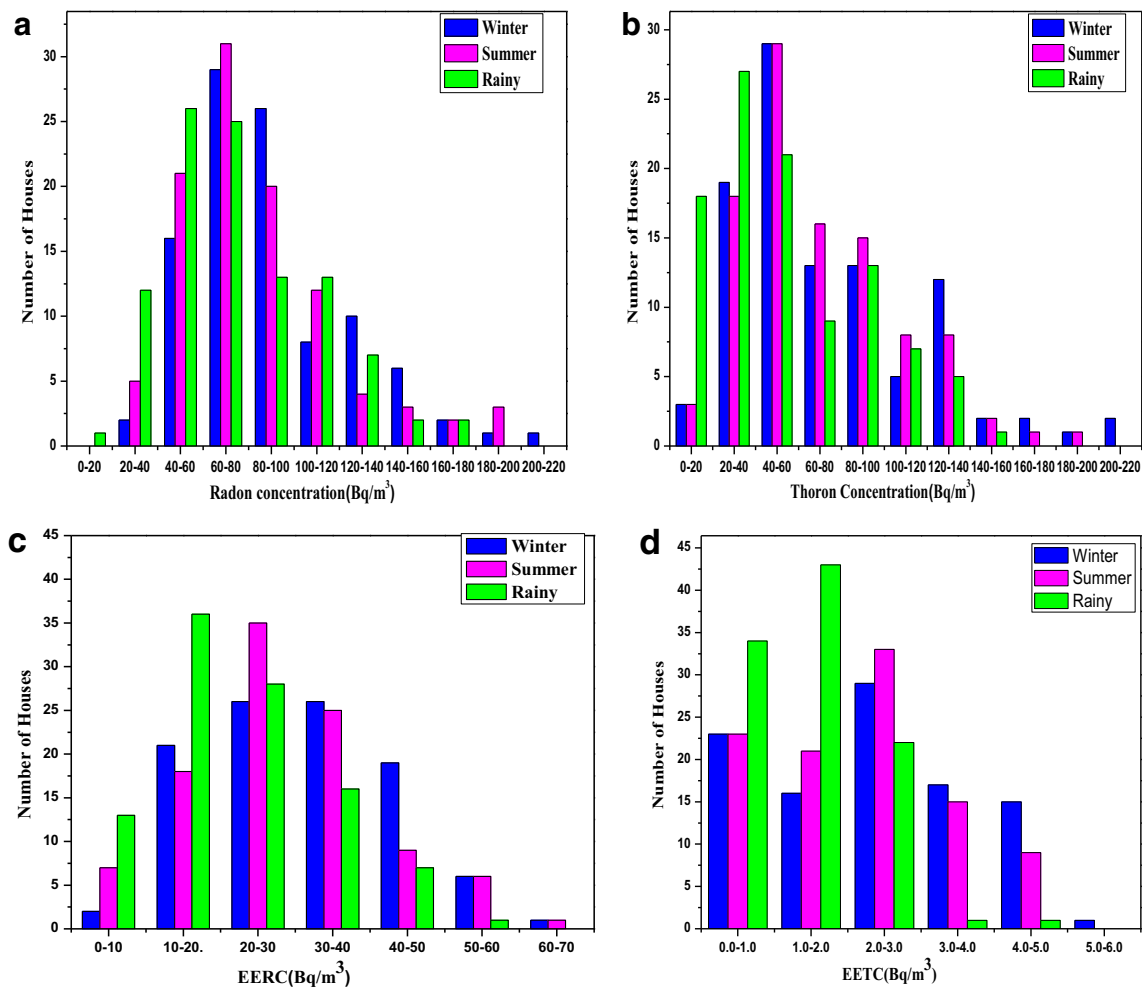


Fig. 3 Sketch of direct <sup>222</sup>Rn/<sup>220</sup>Rn progeny sensors (DRPS/DTPS)



**Fig. 4** **a**  $^{222}\text{Rn}$  frequency distribution curve for all seasons. **b**  $^{220}\text{Rn}$  frequency distribution curve for all seasons. **c** EERC frequency distribution curve for all seasons. **d** EETC frequency distribution curve for all seasons

nanosieverts to millisieverts. Since the equilibrium factors vary with environmental factors, these factors have been estimated independently for individual dwellings.

### Results and discussion

As already discussed,  $^{222}\text{Rn}$ ,  $^{220}\text{Rn}$ , and associated decay products are expected to vary in differing seasons,

dwelling types, and geographic conditions. Air exchange rate plays a vital role in seasonal differences while source term is linked with types of building material and soil. Although such variations have been qualitatively studied in several studies (Cosma et al. 2013), the results cannot be extrapolated to a specific region/context. This section discusses the results obtained from measurements of the above mentioned quantities for the study region.

**Table 1** Statistical data of seasonal variation for indoor  $^{222}\text{Rn}$ ,  $^{220}\text{Rn}$ , and their progeny

| Statistical parameters | $^{222}\text{Rn}$ (Bq/m <sup>3</sup> ) |         |         | $^{220}\text{Rn}$ (Bq/m <sup>3</sup> ) |          |          | EERC (Bq/m <sup>3</sup> ) |          |          | EETC (Bq/m <sup>3</sup> ) |             |             |
|------------------------|--|---------|---------|--|----------|----------|---------------------------|----------|----------|---------------------------|-------------|-------------|
|                        | W                                      | S       | R       | W                                      | S        | R        | W                         | S        | R        | W                         | S           | R           |
| Range                  | 28–217                                 | 27–199  | 14–175  | 13–213                                 | 9–182    | 5–151    | 8–76                      | 6–65     | 3–54     | 0.01–5.36                 | 0.02–4.54   | 0.01–4.02   |
| AM ± SD                | 89 ± 35                                | 83 ± 35 | 75 ± 34 | 73 ± 43                                | 69 ± 37  | 53 ± 35  | 30 ± 13                   | 27 ± 12  | 21 ± 11  | 2.30 ± 1.42               | 2.08 ± 1.31 | 1.39 ± 0.86 |
| RSD                    | 0.39                                   | 0.42    | 0.46    | 0.59                                   | 0.53     | 0.66     | 0.42                      | 0.45     | 0.51     | 0.62                      | 0.63        | 0.62        |
| GM, GSD                | 82, 1.47                               | 77, 1.5 | 67, 1.6 | 61, 1.82                               | 59, 1.81 | 42, 2.11 | 28, 1.61                  | 25, 1.66 | 19, 1.77 | 1.53, 3.24                | 1.62, 2.82  | 0.98, 2.89  |

W winter, S summer, R rainy

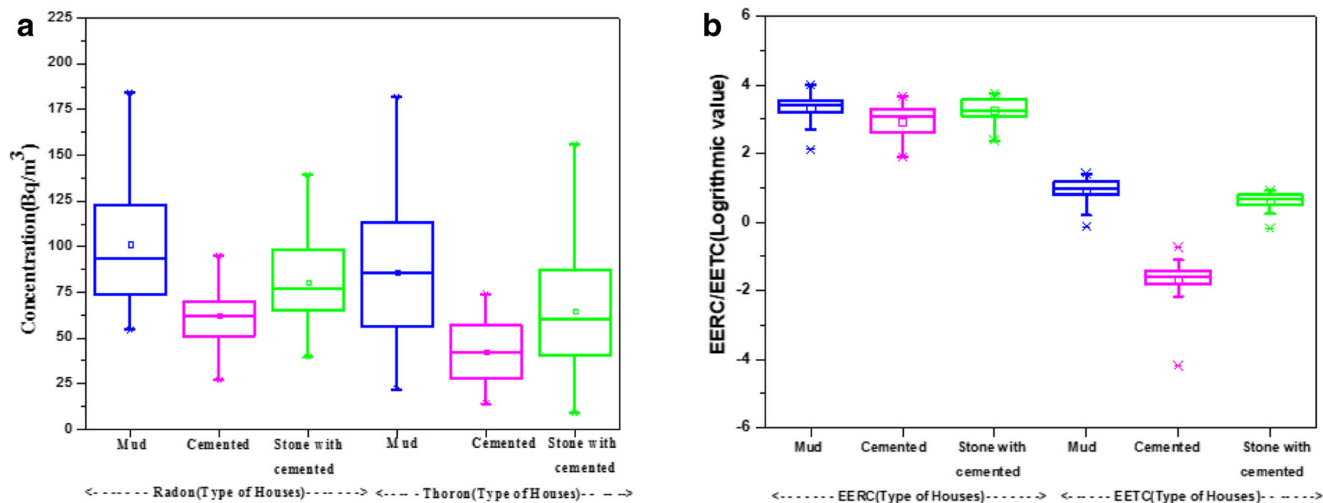


Fig. 5 a Box-Whisker plot of <sup>222</sup>Rn and <sup>220</sup>Rn variations. b Box-Whisker plot of EERC and EETC variations

**Effect of seasons**

Four-month blocks (November to February—winter, March to June—summer, and July to October—rainy) were selected as representing three consecutive seasons (W, S, R) for a year. Daily mean temperature ranges for these blocks (i.e., winter, summer, and rainy) are 13.3–19.4, 21.1–31.1, and 24.5–28.7 °C, respectively. Both gas and progeny dosimeters were deployed in dwellings for each of the above seasons. Figure 4 (a, b) and (c, d) represent the frequency distribution of measured <sup>222</sup>Rn-<sup>220</sup>Rn concentration and EERC-EETC concentration, respectively, in all dwellings for respective seasons.

As can be seen, frequency distribution curves for both <sup>222</sup>Rn and <sup>220</sup>Rn followed lognormal distribution pattern for all seasons. A lognormal distribution function was consequently fitted for individual frequency distributions. Parameters for fitted distributions (geometric mean, GM and geometric standard deviation, GSD) are shown in Table 1. This table also represents arithmetic mean and standard deviation (AM ± SD) and relative standard deviation (RSD) calculated for these distributions. Average values (AM, GM) for the case of <sup>222</sup>Rn were found to be varying in the order of winter > summer > rainy, while dispersion parameters (GSD, RSD) were seen to be relatively higher during the rainy

season. <sup>222</sup>Rn concentrations measured for this region were found to be comparable to other studies conducted in nearby regions (Prasad et al. 2016a, b) as well as with worldwide and Indian average (UNSCEAR 2000). Smaller difference for winter and summer season is possibly due to the offset of ventilation conditions of these seasons. In contrast to general ventilation patterns of cold regions, doors and windows are opened during daytime in winters to allow warm sunlight inside dwellings (except during extreme events such as snowfall). This makes ventilation rates for summers (where air mixing is higher) and winters more or less similar. The number of houses in the higher concentration range (> 100 Bq/m<sup>3</sup> for radon) was found to be more for winters (28) compared to summer (24) and rainy season (24). The increase in dispersion parameters for the rainy season can be explained on the basis of the difference in source term effects for different dwellings. In the rainy season, water fills the pores of soil decreasing exhalation potential and also affects the emission from building material under moist conditions. Such an effect is expected to be different for different types of dwellings thereby increasing dispersion in the rainy season.

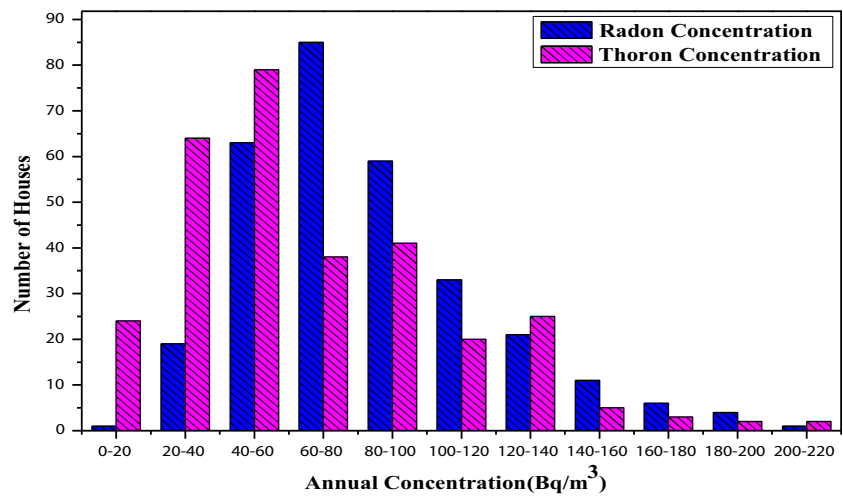
For <sup>220</sup>Rn, relatively lesser effect of ventilation (comparing winter and summer values) was noticed. But similar to the case of <sup>222</sup>Rn, rainy season measured values were

**Table 2** Statistical data of indoor <sup>222</sup>Rn, <sup>220</sup>Rn, and their progeny for different types of dwellings

| Statistical parameters | <sup>222</sup> Rn (Bq/m <sup>3</sup> ) |          |          | <sup>220</sup> Rn (Bq/m <sup>3</sup> ) |          |          | EERC (Bq/m <sup>3</sup> ) |          |          | EETC (Bq/m <sup>3</sup> ) |             |             |
|------------------------|--|----------|----------|--|----------|----------|---------------------------|----------|----------|---------------------------|-------------|-------------|
|                        | M                                      | C        | S        | M                                      | C        | S        | M                         | C        | S        | M                         | C           | S           |
| Range                  | 55–184                                 | 27–95    | 40–139   | 22–182                                 | 14–74    | 9–156    | 8–55                      | 7–39     | 11–42.   | 0.88–4.08                 | 0.02–0.48   | 0.84–2.51   |
| AM ± SD                | 101 ± 36                               | 62 ± 16  | 81 ± 24  | 86 ± 39                                | 42 ± 17  | 64 ± 33  | 31 ± 10                   | 21 ± 9   | 27 ± 8   | 2.66 ± 0.80               | 0.21 ± 0.08 | 1.93 ± 0.42 |
| RSD                    | 0.35                                   | 0.26     | 0.3      | 0.45                                   | 0.39     | 0.52     | 0.33                      | 0.42     | 0.31     | 0.3                       | 0.39        | 0.22        |
| GM, GSD                | 96, 1.42                               | 60, 1.31 | 77, 1.36 | 76, 1.68                               | 39, 1.56 | 56, 1.80 | 29, 1.47                  | 19, 1.63 | 26, 1.39 | 2.53, 1.42                | 0.19, 1.74  | 1.87, 1.29  |

M mud, C cement, S stone with cement

**Fig. 6** Frequency distribution curve for annual  $^{222}\text{Rn}$  and  $^{220}\text{Rn}$  concentration



significantly lesser. The difference in ventilation effects on  $^{222}\text{Rn}$  and  $^{220}\text{Rn}$  concentration has also been highlighted in other studies (Omari et al. 2016; Prasad et al. 2015). Similar arguments as used in the case of  $^{222}\text{Rn}$  explain the lower values and higher dispersion observed in rains. For the case of decay products, frequency distribution plots of EERC and EETC (shown in Fig. 4 c, d) are also lognormal distributed. Mathematically calculated parameters (AM  $\pm$  SD, RSD) and fit-estimated GM are shown in Table 1. As can be noted, seasonal variations in EERC and EETC parameters were similar to the case for that of  $^{222}\text{Rn}$  and  $^{220}\text{Rn}$ . Maximum values for average parameters were obtained in winters as expected. Additionally, values of parameters (range as well as average values) decreased slightly for the rainy season. Increased RSD in the rainy season for EERC and EETC follows the same trend as for their parent gases.

**Effect of building material**

Next, yearly data was segregated on the basis of building type in order to interpret the effect of building material on indoor concentration levels. As already mentioned, sampling was performed in three types of dwellings viz. mud house, cemented house, and stone with cemented house. In each of these houses, sensors were exposed in all three seasons i.e., three readings for each house for an entire year. The distribution of  $^{222}\text{Rn}$ ,  $^{220}\text{Rn}$ , EERC, and EETC for this case has been represented in Fig. 5 (a) and (b) and average parameters are shown in Table 3.

For  $^{222}\text{Rn}$ , average concentration values were found to be significantly lower in cemented houses. Mud houses resulted in higher values of average parameters due to the effect of the source term. In the case of  $^{220}\text{Rn}$ , lower average concentration values were found in the cemented house, similar to the trend for  $^{222}\text{Rn}$ . This trend of lowest averaged values for cemented houses was also followed for EERC and EETC (see Fig. 5 (b) and Table 2). Significantly high exhalation rates and radium/

thorium content for the soil (used as mud in construction of these houses) samples collected from some locations (Semwal et al. 2018) can be attributed to higher values of  $^{222}\text{Rn}$ ,  $^{220}\text{Rn}$ , EERC, and EETC. Apart from that, improper/bare flooring for these houses also contributes towards higher diffusional and convectional flux. In conjunction with the previous section, RSD was also estimated for these cases. RSD was also observed to be affected by the change of building material. It is expected as measured values for each set of dwelling type comprise rainy season concentration values. Lesser concentration values in the cemented house may be attributed to the fact that there is a coating of cement on the floor thereby decreasing the radiation inward flux affecting indoor concentration (Singh et al. 2016a).

**Inferences from yearly data**

After studying the effect of seasons and building material on the measured concentration values, the entire year data was pooled for further deductions. In this way, available 303 data points (three measured values for each dwelling) were grouped for yearly analysis for the study region.

Figure 6 represents the frequency distribution curve for  $^{222}\text{Rn}$  and  $^{220}\text{Rn}$  concentration measured throughout the year. The range of concentration and mean values (calculated and estimated from fitting) are presented in Table 3. These values are compared with results and parameters (wherever

**Table 3** Annual statistical data of  $^{222}\text{Rn}$ ,  $^{220}\text{Rn}$ , and their progeny

| Statistical parameters | $^{222}\text{Rn}$ (Bq/m <sup>3</sup> ) | $^{220}\text{Rn}$ (Bq/m <sup>3</sup> ) | EERC (Bq/m <sup>3</sup> ) | EETC (Bq/m <sup>3</sup> ) |
|------------------------|--|--|---------------------------|---------------------------|
| Range                  | 14–217                                 | 5–213                                  | 3–76                      | 0.01–5.36                 |
| AM $\pm$ SD            | 82 $\pm$ 35                            | 65 $\pm$ 39                            | 26 $\pm$ 13               | 1.92 $\pm$ 1.28           |
| GM, GSD                | 75, 1.53                               | 53, 1.96                               | 23, 1.72                  | 1.30, 3.03                |

**Table 4** Comparison of results of the present study with recent studies conducted for Indian regions

| <sup>222</sup> Rn concentration range (Bq/m <sup>3</sup> ), AM | <sup>220</sup> Rn concentration range (Bq/m <sup>3</sup> ), AM | EERC range, AM (Bq/m <sup>3</sup> ) | EETC range, AM (Bq/m <sup>3</sup> ) | Location                   | References             |
|--|--|-------------------------------------|-------------------------------------|----------------------------|------------------------|
| 10–82 (33)   | 7–180 (79)   | –                                   | –                                   | Haryana                    | Kumar et al. (2015)    |
| 44–157   | 44–240   | 10–63                               | 1–5                                 | Himanchal Pradesh          | Bajwa et al. (2016)    |
| 21–94 (55)   | 17–125 (39)  | 13–57 (25)                          | 0.5–3.5 (1.8)                       | Punjab                     | Bangotra et al. (2015) |
| 25.5–208.5 (63.8)  | 6.7–290 (89.6)   | 12.3–61.2 (29.3)                    | 1.11–6.31 (2.74)                    | Himachal Pradesh           | Singh et al. (2016b)   |
| 21.6–119.5   | 13.5–159   | 7.4–45.7                            | 0.4–4.6                             | Punjab                     | Saini et al. (2016)    |
| 27–148 (54)  | 5–174 (43)   | 7.6–48.6 (19.5)                     | 0.6–4.6 (1.9)                       | Garhwal Himalaya           | Ramola et al. (2016)   |
| 9–58 (28)  | 23–185 (83)  | 5–38 (18)                           | 0.48–5.49 (1.69)                    | Jammu and Kashmir Himalaya | Sharma et al. (2018)   |
| 14–217 (82)  | 5–213 (65)   | 3–76 (26)                           | 0.01–5.36 (1.92)                    | Almora                     | Present study          |

applicable) from other studies conducted in recent times for different Indian regions in Table 4.

As can be seen from Tables 3 and 4, average values of <sup>222</sup>Rn, <sup>220</sup>Rn, EERC, and EETC concentration measured for the study region are higher than the global averages but also comparable to those obtained from other studies in recent times. Observed <sup>222</sup>Rn concentration range (i.e., 14–217 Bq/m<sup>3</sup>) for this study is distinctly towards the upper range reflected in maximum mean value (82 ± 35 Bq/m<sup>3</sup>). Measured <sup>220</sup>Rn concentration (65 ± 39 Bq/m<sup>3</sup>), EERC (26 ± 13 Bq/m<sup>3</sup>), and EETC (1.92 ± 1.28) for the study region was found to be comparable to other study regions but slightly tending towards the higher values. This observation is also consistent when specifically comparing the results of this work with those from measurements made in other

Himalayan/hilly regions. In the absence of data on emanation/exhalation potential and environmental factors, it is not possible to dwell further into the comparative analysis. Nevertheless, the values measured for this region in corroboration with the conclusions of other studies reaffirm the significance of Indian Himalayan belt with respect to background radon/thoron measurements.

A close look at Fig. 6 suggests that indoor <sup>222</sup>Rn and <sup>220</sup>Rn concentration crossed 100 Bq/m<sup>3</sup> for a significant number of houses. To dwell further, Pie charts (Fig. 7) are drawn for measured yearly gas and decay product concentration values. It can be visualized from these plots that a total of 60.07, 20.79, 3.96, and 0.03% and 38.61, 15.84, 2.31, and 0.66% houses correspond to measurement ranges 50–100, 100–150, 150–200, and 200–250 Bq/m<sup>3</sup> of <sup>222</sup>Rn and <sup>220</sup>Rn

**Fig. 7** Pie chart for concentration of <sup>222</sup>Rn, <sup>220</sup>Rn, and their decay products

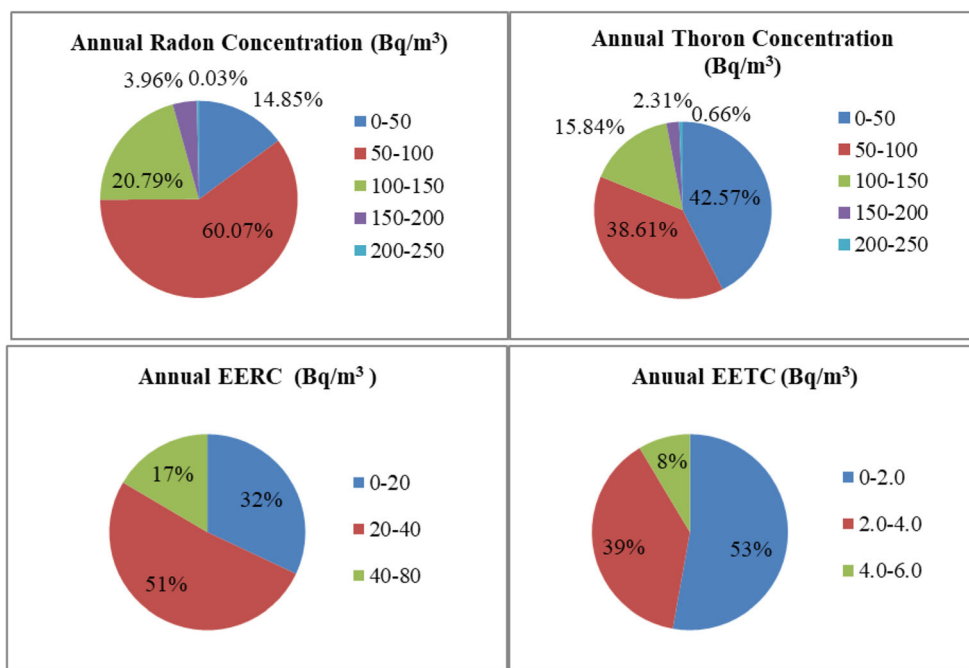




**Table 5** Range and the average value of equilibrium factor and annual inhalation dose due to indoor  $^{222}\text{Rn}/^{220}\text{Rn}$

|             | Equilibrium factor                |                                   | Annual effective dose (mSv/y)     |                                   | AID (mSv/y)     |
|-------------|-----------------------------------|-----------------------------------|-----------------------------------|-----------------------------------|-----------------|
|             | $^{222}\text{Rn}$ and its progeny | $^{220}\text{Rn}$ and its progeny | $^{222}\text{Rn}$ and its progeny | $^{220}\text{Rn}$ and its progeny |                 |
| Range       | 0.12–0.82                         | 0.001–0.24                        | 0.42–3.49                         | 0.004–1.14                        | 0.55–4.71       |
| AM $\pm$ SD | 0.34 $\pm$ 0.14                   | 0.037 $\pm$ 0.035                 | 1.67 $\pm$ 0.64                   | 0.54 $\pm$ 0.29                   | 2.36 $\pm$ 0.83 |

concentration, respectively. For the case of  $^{222}\text{Rn}$ , measured concentration values were higher than the reference level of 100 Bq/m<sup>3</sup> (WHO 2009) in 25% dwellings of the study region. For  $^{220}\text{Rn}$ , 19% and 38% of dwellings showed concentration values higher than 100 and 50 Bq/m<sup>3</sup> (arbitrary chosen references), respectively. For EERC and EETC, 49% and 50% of dwellings were observed having concentrations higher than yearly averaged 26 and 1.92 (median) value, respectively.  $^{220}\text{Rn}$  activity concentration and EETC were found to be significantly higher than global indoor average for this region. This is due to high thoron surface exhalation rates (0.65–6.43 Bq/m<sup>2</sup>/sec) and thorium content (27.46–89.00 Bq/kg) measured from soil samples collected from some of the locations from this region (Semwal et al. 2018). A separate elaborative study is being conducted in this study region specifically targeting high concentration houses to investigate the reason for the same. As a final step, equilibrium factor and annual effective doses (due to radon, thoron, and combined) are estimated for the study region (using Eqs. (1), (2), (3), (4), and (5)). These values are summarized in the form of Table 5.

Although EF for  $^{222}\text{Rn}$  and its progeny were found to vary from 0.12–0.82, yearly averaged value (i.e., 0.34  $\pm$  0.14) was close to the reference value (0.4) for the outdoor environment. On the contrary, EF for  $^{220}\text{Rn}$  and its decay products was estimated to be a bit higher (0.037  $\pm$  0.035) in comparison to its reference value (0.02) but with large uncertainty. Annual effective dose due to  $^{222}\text{Rn}$  and  $^{220}\text{Rn}$  calculated for the study region was found to be 1.67  $\pm$  0.64 and 0.54  $\pm$  0.29 mSv/y, respectively. Annual inhalation dose due to  $^{222}\text{Rn}$ ,  $^{220}\text{Rn}$ , and their progeny were found to be 0.55–4.71 mSv/y with an average value of 2.36  $\pm$  0.83. These values (i.e., EF and AID) are also compared with deductions made in recent studies carried out in nearby regions in Table 6. It can be seen that

these values are comparable to values obtained from other studies and compilation report (ICRP 2011).

### Conclusions

This study was conducted in 101 dwellings of different construction materials situated at different villages in Almora District, Uttarakhand, located in Indian Himalayan belt.  $^{222}\text{Rn}$ ,  $^{220}\text{Rn}$ , and their decay product’s concentration were measured by using a single entry pin-hole-based dosimeter and DRPS/DTPS, respectively. The measurement campaign was conducted in the entire year covering winter, summer, and rainy seasons. For the case of  $^{222}\text{Rn}$ , average concentration values were found higher in winter season followed by summer and rainy season. The role of ventilation and source flux reduction in rains has been discussed. For  $^{220}\text{Rn}$ , concentration values were lesser for rainy season but similar for other two seasons. An interesting observation pertains to higher relative standard deviation (RSD) noticeable for rainy season for both  $^{222}\text{Rn}$  and  $^{220}\text{Rn}$ . Reduction of the source term in rains is expected to be different for different construction material thereby increasing dispersion characteristics. Seasonal variations of EERC and EETC were found to be following their parent gases. For  $^{222}\text{Rn}/^{220}\text{Rn}$  (and EERC/ EETC), average concentration values were found to be varying as per the order: mud > stone with stone > cement houses based on the construction material of dwellings. Lesser concentration values in the cemented house may be due to the coating of cement on the floor causing a decrease in the radiation inward flux. Twenty-five percent dwellings of study region were found to be having  $^{222}\text{Rn}$  concentration more than 100 Bq/m<sup>3</sup> averaged for the entire year. For  $^{220}\text{Rn}$ , 19% and 38% of

**Table 6** Comparison of equilibrium factor and dose results of the present study with other Indian studies

| Equilibrium factor range, AM      |                                   | AID, AM (mSv/y)  | References           |
|-----------------------------------|-----------------------------------|------------------|----------------------|
| $^{222}\text{Rn}$ and its progeny | $^{220}\text{Rn}$ and its progeny |                  |                      |
| 0.10–0.62 (0.4)                   | 0.02–0.17 (0.07)                  | 0.8–4.6, 1.8     | Ramola et al. (2016) |
| 0.12–0.77 (0.50)                  | 0.01–0.34 (0.05)                  | –                | Singh et al. (2016b) |
| 0.15–0.95 (0.45)                  | 0.01–0.16 (0.04)                  | 1.1–4.1 (2.4)    | Saini et al. (2016)  |
| 0.12–0.82 (0.34)                  | 0.001–0.24 (0.037)                | 0.55–4.71 (2.36) | Present study        |

dwellings showed concentration values higher than 100 Bq/m<sup>3</sup> and 50 Bq/m<sup>3</sup>, respectively. Measured EERC and EETC were found to be higher than yearly averaged value i.e., 26 and 1.92 for 49% and 50% dwellings, respectively. High exhalation potential and radioactivity content in the soil samples collected from some locations of the study region could be attributed to the observed concentration values. Yearly averaged value of equilibrium factor (EF) estimated for <sup>222</sup>Rn and its progeny and <sup>220</sup>Rn and its progeny was 0.34 ± 0.14 and 0.037 ± 0.035, respectively. Average effective dose due to <sup>222</sup>Rn and <sup>220</sup>Rn was calculated to be 1.67 ± 0.64 and 0.54 ± 0.29 mSv/y, respectively. Annual inhalation dose due to <sup>222</sup>Rn, <sup>220</sup>Rn, and their progeny was found to be 0.55–4.71 mSv/y with an average value of 2.36 ± 0.83 mSv/y. These radiation doses are comparable with other Indian results in nearby regions in recent times. The elaborative findings from this study are important for Indian database for indoor <sup>222</sup>Rn/<sup>220</sup>Rn exposure.

**Funding information** The authors are thankful to the Board of Research in Nuclear Science (BRNS), Department of atomic energy (DAE), Mumbai, India, for providing the funds (project no. 2013/36/61-BRNS) and the facilities for carrying out the research work.

## References

- Agarwal TK, Sahoo BK, Gaware JJ, Joshi M, Sapra BK (2014) CFD based simulation of thoron (<sup>220</sup>Rn) concentration in a delay chamber for mitigation application. *J Environ Radioact* 136:16–21. <https://doi.org/10.1016/j.jenvrad.2014.05.003>
- Agarwal TK, Joshi M, Sahoo BK, Kanse SD, Sapra BK (2016) Effect of <sup>220</sup>Rn gas concentration distribution on its transmission from a delay chamber: evolving a CFD-based uniformity index. *Radiat Prot Dosim* 168:546–552. <https://doi.org/10.1093/rpd/ncv361>
- Bajwa BS, Singh P, Singh P, Saini K, Singh S, Sahoo BK, Sapra BK (2016) A follow-up study on indoor <sup>222</sup>Rn, <sup>220</sup>Rn their decay product concentrations in a mineralised zone of Himachal Pradesh, India. *Radiat Prot Dosim* 168:553–560. <https://doi.org/10.1093/rpd/ncv367>
- Bangotra P, Mehra R, Kaur K, Kanse S, Mishra R, Sahoo BK (2015) Estimation of EEC, unattached fraction and equilibrium factor for the assessment of radiological dose using pin-hole cup dosimeters and deposition based progeny sensors. *J Environ Radioact* 148:67–73. <https://doi.org/10.1016/j.jenvrad.2015.06.010>
- Barros-Diosa JM, Ruano-Ravina A, Gastelu-Iturrid CJ, Figueiras A (2007) Factors underlying residential radon concentration: results from Galicia, Spain. *Environ Res* 103:185–190. <https://doi.org/10.1016/j.envres.2006.04.008>
- Br EV, Andersen CE, Sørensen M, Jovanovic Z, Gravesen P, Ulbak K, Hertel O, Pedersen C, Overvad K, Tjønneland A, Raaschou-Nielsen O (2012) Residential radon and lung cancer incidence in a Danish cohort. *Environ Res* 118:130–136. <https://doi.org/10.1016/j.envres.2012.05.012>
- Chauhan N, Chauhan RP, Joshi M, Agarwal TK, Aggarwal P, Sahoo BK (2014) Study of indoor radon distribution using measurements and CFD modeling. *J Environ Radioact* 136:105–111. <https://doi.org/10.1016/j.jenvrad.2014.05.020>
- Chauhan N, Chauhan RP, Joshi M, Agarwal TK, Sapra BK (2015) Measurements and CFD modeling of indoor thoron distribution. *Atmos Environ* 105:7–13. <https://doi.org/10.1016/j.atmosenv.2015.01.029>
- Cosma C, Cucos A, Papp B, Begy R, Sainz C (2013) Soil and building material as main sources of indoor radon in Baita-Steiradon prone area (Romania). *J Environ Radioact* 116:174–179. <https://doi.org/10.1016/j.jenvrad.2012.09.006>
- Harris SA, Billmeyer ER, Robinson MA (2006) Evaluation of repeated measurements of radon-222 concentrations in well water sampled from bedrock aquifers of the Piedmont near Richmond, Virginia, USA: effects of lithology and well characteristics. *Environ Res* 101:323–333. <https://doi.org/10.1016/j.envres.2006.02.002>
- İçhedef M, Saç MM, Camgöz B, Bolca M, Harmansah Ç (2013) Soil gas radon concentrations measurements in terms of great soil groups. *J Environ Radioact* 126:165–171. <https://doi.org/10.1016/j.jenvrad.2013.08.003>
- International Commission on Radiological Protection, ICRP (2011) Lung cancer risk from radon and progeny and statement on radon. ICRP Publication-115. Pergamon Press. In: Oxford
- Irlinger J, Wielunski M, Rühm W (2014) Thoron detection with an active radon exposure meter—first results. *Rev Sci Instrum* 85(2):022106. <https://doi.org/10.1063/1.4865162>
- Jelle BP (2012) Development of a model for radon concentration in indoor air. *Sci Total Environ* 416:343–350. <https://doi.org/10.1016/j.scitotenv.2011.11.052>
- Jelle BP, Noreng K, Erichsen THST (2011) Implementation of radon barriers, model development and calculation of radon concentration in indoor air. *J Build Phys* 34:195–222. <https://doi.org/10.1177/1744259109358285>
- Jeon HJ, Kang DR, Go SB et al (2017) A preliminary study for conducting a rational assessment of radon exposure levels. *Environ Sci Pollut Res* 24:14491. <https://doi.org/10.1007/s11356-017-9030-5>
- Joshi M, Sapra BK, Khan A, Kothalkar P, Mayya YS (2010) Thoron (<sup>220</sup>Rn) decay products removal in poorly ventilated environments using unipolar ionizers: dosimetric implications. *Sci Total Environ* 408:5701–5706. <https://doi.org/10.1016/j.scitotenv.2010.08.011>
- Joshi M, Sapra BK, Kothalkar P, Khan A, Modi R, Mayya YS (2011) Implications of polarity of unipolar ionisers on reduction of effective dose attributable to thoron progeny. *Radiat Prot Dosim* 145(2-3): 256–259. <https://doi.org/10.1093/rpd/ncr063>
- Kumar A, Chauhan RP, Joshi M, Sahoo BK (2014) Modeling of indoor radon concentration from radon exhalation rates of building materials and validation through measurements. *J Environ Radioact* 127: 50–55. <https://doi.org/10.1016/j.jenvrad.2013.10.004>
- Kumar A, Chauhan RP, Joshi M, Aggarwal P (2015) Implications of variability in Indoor radon/thoron levels: a study of dwellings in Haryana, India. *Environ Earth Sci* 73(8):4033–4042. <https://doi.org/10.1007/s12666>
- Mayya YS, Mishra R, Prajith R, Sapra BK, Kushwaha HS (2010) Wire-mesh capped deposition sensors: novel passive tool for coarse fraction flux estimation of radon thoron progeny in indoor environments. *Sci Total Environ* 409:378–383. <https://doi.org/10.1016/j.scitotenv.2010.10.007>
- Meisenberg O, Mishra R, Joshi M, Gierl S, Rout R, Guo L, Agarwal T, Kanse S, Irlinger J, Sapra BK, Tschiersch J (2016) Radon and thoron inhalation doses in dwellings with earthen architecture: comparison of measurement methods. *Sci Total Environ* 579:1855–1862. <https://doi.org/10.1016/j.scitotenv.2016.11.170>
- Mishra R, Mayya YS (2008) Study of a deposition-based direct thoron progeny sensor (DTPS) technique for estimating equilibrium equivalent thoron concentration (EETC) in indoor environment. *Radiat Meas* 43:1408–1416. <https://doi.org/10.1016/j.radmeas.2008.03.002>
- Mishra R, Mayya YS, Kushwaha HS (2009a) Measurement of <sup>220</sup>Rn/<sup>222</sup>Rn progeny deposition velocities on surfaces and their

- comparison with theoretical models. *J Aerosol Sci* 40:1–15. <https://doi.org/10.1016/j.jaerosci.2008.08.001>
- Mishra R, Sapra BK, Mayya YS (2009b) Nuclear instruments and methods in physics research B development of an integrated sampler based on direct  $^{222}\text{Rn}/^{220}\text{Rn}$  progeny sensors in flow-mode for estimating unattached/attached progeny concentration. *Nucl Inst Methods Phys Res B* 267:3574–3579. <https://doi.org/10.1016/j.nimb.2009.08.021>
- Mishra R, Prajith R, Sapra BK, Mayya YS (2010) Nuclear instruments and methods in physics research B response of direct thoron progeny sensors (DTPS) to various aerosol concentrations and ventilation rates. *Nucl Inst Methods Phys Res B* 268:671–675. <https://doi.org/10.1016/j.nimb.2009.12.012>
- Mishra R, Zunic ZS, Venoso G et al (2014) An evaluation of thoron (and radon) equilibrium factor close to walls based on long-term measurements in dwellings. *Radiat Prot Dosim* 160(1-3):164–168. <https://doi.org/10.1093/rpd/ncu083>
- Nikezic D, Yu KN (2005) Are radon gas measurements adequate for epidemiological studies and case control studies of radon-induced lung cancer? *Radiat Prot Dosim* 113:233–235. <https://doi.org/10.1093/rpd/nch451>
- Omori Y, Prasad G, Sorimachi A, Kumar S, Ishikawa T, Vidya D, Chand R, Tokonami S (2016) Long-term measurements of residential radon, thoron, and thoron progeny concentrations around the Chhatrapur placer deposit, a high background radiation area in Odisha, India. *J Environ Radioact* 162:371–378. <https://doi.org/10.1016/j.jenvrad.2016.06.009>
- Park TH, Kang DR, Park SH et al (2018) Indoor radon concentration in Korea residential environments. *Environ Sci Pollut Res*. <https://doi.org/10.1007/s11356-018-1531-3>
- Prasad G, Prasad Y, Gusain GS, Ramola RC (2008a) Measurement of radon and thoron levels in soil, water and indoor atmosphere of Budhakedar in Garhwal Himalaya, India. *Radiat Meas* 43:375–379. <https://doi.org/10.1016/j.radmeas.2008.04.050>
- Prasad Y, Prasad G, Gusain GS, Choubey VM, Ramola RC (2008b) Radon exhalation rate from soil samples of South Kumaun Lesser Himalayas. *India Radiat Meas* 43:369–374. <https://doi.org/10.1016/j.radmeas.2008.04.056>
- Prasad M, Rawat M, Dangwal A, Yadav M, Gusain GS, Mishra R, Ramola RC (2015) Measurements of radon and thoron progeny concentrations in dwellings of Tehri Garhwal, India, using LR-115 deposition-based DTSP/DRPS technique. *Radiat Prot Dosim* 167(1-3):102–106. <https://doi.org/10.1093/rpd/ncv224>
- Prasad M, Rawat M, Dangwal A, Prasad G, Mishra R, Ramola RC (2016a) Study of indoor radon, thoron and progeny in the indoor environment of Yamuna and Tons valleys of Garhwal Himalaya and progeny in the indoor environment of Yamuna. *Sci Rep* 6. <https://doi.org/10.1090/rpd/ncw055>
- Prasad M, Rawat M, Dangwal A, Kandari T, Gusain GS, Mishra R, Ramola RC (2016b) Variability of radon and thoron equilibrium factors in indoor environment of Garhwal Himalaya. *J Environ Radioact* 151:238–243. <https://doi.org/10.1016/j.jenvrad.2015.10.017>
- Ramola RC, Negi MS, Choubey VM (2003) Measurement of equilibrium factor “F” between radon and its progeny and thoron and its progeny in the indoor atmosphere using nuclear track detectors. *Indoor Built Environ* 12(5):351–355. <https://doi.org/10.1177/142032603035368>
- Ramola RC, Negi MS, Choubey VM (2005) Radon and thoron monitoring in the environment of Kumaun Himalayas: survey and outcomes. *J Environ Radioact* 79:85–92. <https://doi.org/10.1016/j.jenvrad.2004.05.012>
- Ramola RC, Prasad G, Gusain GS, Rautela BS, Sagar DV, Tokonami S, Sorimachi A, Sahoo SK, Janik M, Ishikawa T, Thaul B (2010) Preliminary indoor thoron measurements in high radiation background area of southeastern coastal Orissa, India. *Radiat Prot Dosim* 141:379–382. <https://doi.org/10.1093/rpd/ncq238>
- Ramola RC, Rautela BS, Gusain GS, Prasad G, Sahoo SK, Tokonami S (2013) Measurements of radon and thoron concentrations in high radiation background area using pin-hole dosimeter. *Radiat Meas* 53:71–73. <https://doi.org/10.1016/j.radmeas.2013.04.008>
- Ramola RC, Prasad M, Kandari T, Pant P, Bossew P, Mishra R, Tokonami S (2016) Dose estimation derived from the exposure to radon, thoron and their progeny in the indoor environment. *Sci Rep* 6
- Ryzhakova NK (2012) Parameters of modeling radon transfer through soil and methods of their determination. *J Appl Geophys* 80:151–157. <https://doi.org/10.1016/j.jappgeo.2012.01.010>
- Sahoo BK, Mayya YS (2010) Two dimensional diffusion theory of trace gas emission into soil chambers for flux measurements. *Agric For Meteorol* 150:1211–1224. <https://doi.org/10.1016/j.agrformet.2010.05.009>
- Sahoo BK, Mayya YS, Sapra BK, Gaware JJ, Banerjee KS, Kushwaha HS (2010) Radon exhalation studies in an Indian uranium tailings pile. *Radiat Meas* 45(2). <https://doi.org/10.1016/j.radmeas.2010.01.008>
- Sahoo BK, Sapra BK, Gaware JJ, Kanse SD, Mayya YS (2011) A model to predict radon exhalation from walls to indoor air based on the exhalation from building material samples. *Sci Total Environ* 409:2635–2641. <https://doi.org/10.1016/j.scitotenv.2011.03.031>
- Sahoo BK, Sapra BK, Kanse SD, Gaware JJ, Mayya YS (2013) A new pin-hole discriminated  $^{222}\text{Rn}/^{220}\text{Rn}$  passive measurement device with single entry face. *Radiat Meas* 58:52–60. <https://doi.org/10.1016/j.radmeas.2013.08.003>
- Sahoo BK, Agarwal TK, Gaware JJ, Sapra BK (2014) Thoron interference in radon exhalation rate measured by solid state nuclear track detector based can technique. *J Radioanal Nucl Ch* 302:1–4. <https://doi.org/10.1007/s10967-014-3580-5>
- Saini K, Sahoo BK, Bajwa BS (2016) Estimation of indoor radon, thoron and their decay products’ concentrations along with annual inhalation dose in dwellings of Punjab, India. *Indoor Built Environ*, 1420326X16676305. <https://doi.org/10.1177/1420326X16676305>
- Semwal P, Singh K, Agarwal TK, Joshi M, Pant P, Kandari T, Ramola RC (2018) Measurement of  $^{222}\text{Rn}$  and  $^{220}\text{Rn}$  exhalation rate from soil samples of Kumaun Hills, India. *Acta Geophysica*:1–9. <https://doi.org/10.1007/s11600-018-0124-3>
- Sharma S, Kumar A, Mehra R, Kaur M, Mishra R (2018) Assessment of progeny concentrations of  $^{222}\text{Rn}/^{220}\text{Rn}$  and their related doses using deposition-based direct progeny sensors. *Environ Sci Pollut Res* 8:1–4. <https://doi.org/10.1007/s11356-018-1414-7>
- Singh K, Semwal P, Pant P, Gusain GS, Joshi M, Sapra BK, Ramola RC (2016a) Measurement of radon, thoron and their progeny in different types of dwelling in Almora district of Kumaun Himalayan region. *Radiat Prot Dosim* 171:223–228. <https://doi.org/10.1093/rpd/new063>
- Singh P, Saini K, Mishra R, Kumar B (2016b) Attached, unattached fraction of progeny concentrations and equilibrium factor for dose assessments from  $^{222}\text{Rn}$  and  $^{220}\text{Rn}$ . *Radiat Environ Biophys*. <https://doi.org/10.1007/s00411-016-0656-3>
- Sonkawade RG, Kant K, Muralithar S, Kumar R, Ramola RC (2008) Natural radioactivity in common building construction and radiation shielding materials. *Atmos Environ* 42(9):2254–2259. <https://doi.org/10.1016/j.atmosenv.2007.11.037>
- Teras LR, Diver WR, Turner MC, Krewski D, Sahar L, Ward E, Gapstur SM (2016) Residential radon exposure and risk of incident hematologic malignancies in the Cancer Prevention Study-II Nutrition Cohort. *Environ Res* 148:46–54. <https://doi.org/10.1016/j.envres.2016.03.002>
- United Nations Scientific Committee on the Effect of Atomic Radiation, UNSCEAR (1993) Effects and risks of ionizing radiation. United Nations, New York
- United Nations Scientific Committee on the Effect of Atomic Radiation, UNSCEAR (2008) Sources and effects of ionizing radiation. United Nations, New York

- United Nations Scientific Committee on the Effect of Atomic Radiation, UNSCEAR (2010) Sources and effects of ionizing radiation. UNSCEAR 2008 Report Volume I:Sources. United Nations, New York
- United Nations Scientific Committee on the Effects of Atomic Radiation, UNSCEAR (2000) Sources and effects of ionizing radiation. Report Volume I:Sources. United Nations, New York
- Valdia KS (1963) The stratigraphy and structure of the Lohaghat subdivision, district Almora, U.P. Q. JI. geol. Min metal Soc, India 35: 165–185
- Vasilyev AV, Zhukovsky MV (2013) Determination of mechanisms and parameters which affect radon entry into a room. *J Environ Radioact* 124:185–190. <https://doi.org/10.1016/j.jenvrad.2013.04.014>
- Wang F, Ward IC (2000) The development of a radon entry model for a house with a cellar. *Build Environ* 35:615–631. [https://doi.org/10.1016/S0360-1323\(99\)00052-9](https://doi.org/10.1016/S0360-1323(99)00052-9)
- World Health Organization, WHO (2009) Hand book on indoor radon: a public health perspective. WHO Press, Geneva